International Journal of Thermophysics, Vol. 7, No. 4, 1986

Measurement of the Effective Thermal Conductivity of Agricultural Products[1]

H. Inaba[2]

This paper reports new measurements of the effective thermal conductivity of agricultural materials such as grains by means of the transient heat flow method using a line heat source. The effect of a probe diameter used for the transient heat flow method on the effective thermal conductivity was studied using standard spherical particles and some grains. It was concluded that the transient heat flow method can be applied to the measurement of the effective thermal conductivity of agricultural materials such as grains provided that the ratio of the probe diameter to the diameter of the particles of the specimen is greater than unity.

KEY WORDS: agricultural materials; effective thermal conductivity; guarded hot-plate method; line heat source; transient heat flow method.

1. INTRODUCTION

In recent years, it has become necessary for the agricultural industry to obtain fundamental information on thermophysical properties of agricultural materials in order to estimate the energy requirements for long-time storage and to analyze the relevant processes such as drying, cooling, and aeration. Thermal conductivity is one of the most important properties needed in the design or control of an agricultural material storage equipment and treatment system. Measurement of the thermal conductivity of agricultural materials is difficult because they are composed of different constituents, for example, water, air, and solid constituents (protein, fats, carbohydrate, ash, etc.), and have a porous structure. The

[1] Invited paper presented at the Ninth Symposium on Thermophysical Properties, June 24–27, 1985, Boulder, Colorado, U.S.A.

[2] Department of Mechanical Engineering, Kitami Institute of Technology, Koen-Cho 165, Kitami, Hokkaido 090, Japan.

0195-928X/86/0700-0773$04.00/0

effective thermal conductivity of grains as an agricultural materials has been measured by the steady-state guarded hot-plate method [1–5]. However, this method requires a very long measurement time. This long measurement time causes changes to take place in the agricultural materials. Therefore, the measurement of thermal conductivity by means of the guarded hot-plate method requires the greatest care. Instead of the guarded hot-plate method used previously for agricultural materials, the present study attempts to apply the transient heat flow method [6] using a line heat source (which has been used to measure the thermal conductivity of fluids and powders having a homogeneous structure) to the measurement of the effective thermal conductivity of agricultural materials such as grains having a porous structure. This transient heat flow method has some merits: it enables the measurement of the effective thermal conductivity of agricultural materials before they undergo changes because of the very short measurement time, and the heat loss from the measuring device becomes negligibly small due to the line heat source. However, for measurement of the effective thermal conductivity of grains having a porous structure, it will be assumed that the geometrical and thermal nonhomogenity of measuring specimens around the probe, used for the transient heat flow method, depends on the number of contact points of the particles of the specimen to the probe surface. Therefore, this nonhomogenity suggests the existence of optimum regions of the geometrical dimension of the probe and particles of the specimen, heat flux added to the probe and measuring time depending on the heat capacity of the probe, thermal properties of the specimen, and natural convection of the air layer near the probe.

The primary purpose of the present study is to examine the limitation of the geometrical dimension of the probe and of the specimen when the effective thermal conductivity of the agricultural materials, such as grains, is measured by means of the transient heat flow method using a line heat source. The experiments for the transient heat flow method are performed using standard spherical materials of known thermal conductivity. The results obtained by the transient heat flow method are compared with those obtained by the guarded hot-plate method.

2. EXPERIMENTAL

2.1. Guarded Hot-Plate Method

A schematic diagram of the experimental apparatus is shown in Fig. 1. The main parts of the apparatus are a heating part placed at the upper side, a test section, and a cooling part placed at the lower side. The effec-

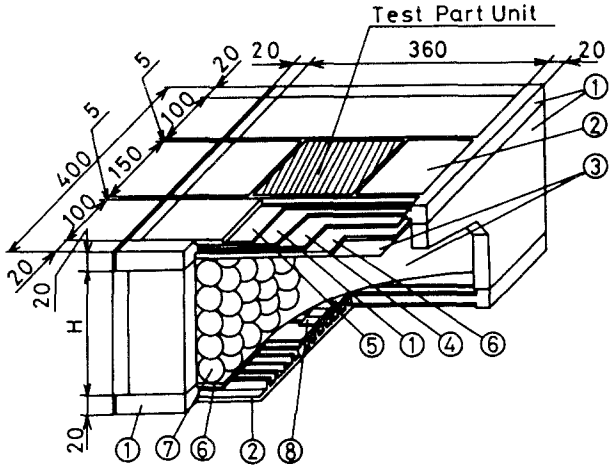

Fig. 1. Schematic diagram of the experimental apparatus for the guarded hot-plate method.

tive thermal conductivity of the specimen was masured in the rectangular test space packed with the specimen, $150 \times 150 \times H$ mm (where H is the distance between the hot and the cold walls), in the middle part as shown in Fig. 1. In order to minimize the heat loss from the test section to the environment, the test section was surrounded by guards 100 mm in width. A sectional view of the apparatus is shown in Fig. 2. The heating part consists of a hot wall (copper plate of 6-mm thickness), the main mica electric heater (maximum power output of 1 kW), and a guarded mica electric heater mounted outside the main heater across a Bakelite plate. The surface temperature of the hot wall was controlled to within ± 0.1°C of the desired temperature. The cooling part was constructed of a cold wall (copper plate 6 mm in thickness) and a water jacket was attached to the outside of the cold wall. The surface temperature of the cold wall was controlled to within ± 0.1°C of the desired temperature. The distance, H, between the hot and the cold walls was adjustable in the range 50 to 100 mm, depending on the diameter of the specimen particles used. In order to attain a good contact between the speciment and the hot and cold walls, the particles were packed in an orderly fashion from an entrance of the upper side wall of the experimental apparatus rotated vertically by a turn-

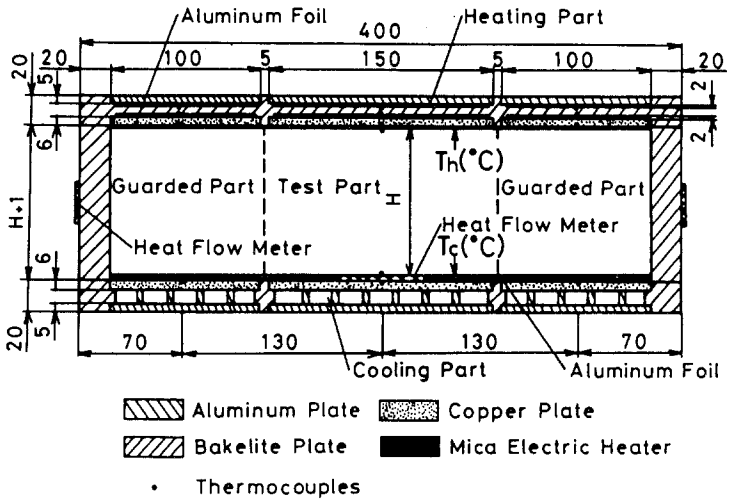

Fig. 2. Sectional view of the apparatus shown in Fig. 1.

ing stand. In order to lessen the radiative heat transfer, thin aluminum foils (10 μm in thickness) with a low thermal emissivity ($=0.06$) were attached to the hot and cold walls, and the temperature difference between the two walls was controlled to within 10°C.

To minimize the heat loss, the apparatus was covered with styrofoam insulating material 100 mm in thickness and was placed in a temperature-controlled room. The room temperature was set to a value corresponding to the average of the surface temperatures of the hot and the cold walls. The heat loss measured by the heat flow meters, mounted on the side walls, was within $\pm 1\%$ of the total heat flow through the specimen. The effective thermal conductivity, λ_{eff}, of the specimen is calculated by the following equation:[3]

$$\lambda_{\text{eff}} = \frac{QH}{A(T_{\text{h}} - T_{\text{c}})} \tag{1}$$

The net heat flow Q through the specimen was obtained from the measurements with the heat flow meters mounted on the cold wall.

Alumina balls of various diameters and glass beads were used as standard spherical solid particles; their mean diameters and thermophysical

[3] For an explanation of symbols, see Nomenclature at the end of the article.

Table I. Geometrical and Thermophysical Properties for Standard Spherical Materials

	Mean diameter (mm)	Dnsity ($kg \cdot m^{-3}$)	Specific heat ($kJ \cdot kg^{-1} \cdot K^{-1}$)	Thermal conductiving ($W \cdot m^{-1} \cdot K^{-1}$)	Mean deviation (mm)
Alumina	0.971	3560	0.84	15.9	0.0715
	5.11				0.1995
	10.2				0.3516
	21.2				0.2468
Glass beads	5.40	2450	0.75	0.74	0.2813

properties are given in Table I. Four kinds of grains, that is, rice, adzuki beans, soy beams and tora beams, were used as agricultural materials; their hydrodynamic diameters and constituents are presented in Table II.

2.2. Transient Heat Flow Method

A schematic diagram of the cylindrical apparatus is shown in Fig. 3. It is constructed in order to measure the effective thermal conductivity of agricultural materials such as grains by means of the transient heat flow method using a line heat source. The specimen was packed in an orderly fashion into a steel cylinder 400 mm in internal diameter and 500 mm in height from the upper end. The temperature of the cylindrical test part was controlled in the temperature range 10 to 90°C by a temperature-controlled water water jacket attached to the outside of the steel cylinder. As a result, it was possible to control the radial temperature distribution of the test section to within 4×10^{-3} °C $\cdot$ cm^{-1}. The probe for the transient heat flow method was placed centrally inside the steel cylinder as shown in

Table II. Geometrical and Thermophysical Properties for Grains Used

	Equivalent diameter (mm)	Density ($kg \cdot m^{-3}$)	Water (%)	Protein (%)	Fats (%)	Carbohydrate		Aash (%)
						Sugar (%)	Fiber (%)	
Rice	2.91	1419	15.5	6.6	0.8	76.6	0.3	0.6
Soy beans	7.11	1225	12.0	34.2	17.5	26.7	4.5	5.0
Adzuki beans	5.37	1302	15.5	21.5	1.6	54.1	4.3	3.0
Tora beans	10.1	1301	16.0	20.2	2.2	54.3	3.7	3.6

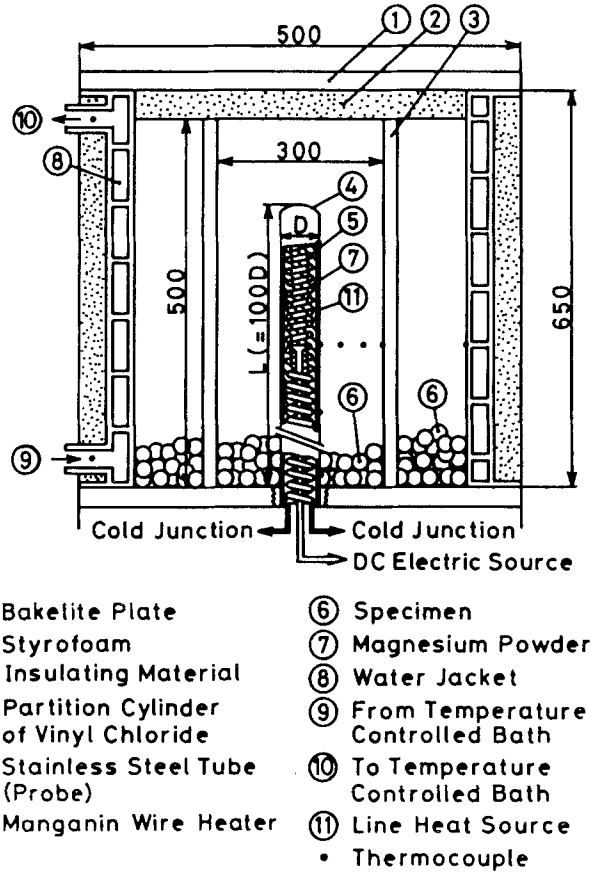

Fig. 3. Schematic diagram of the apparatus for the transient heat flow method.

Fig. 3. The probe, attached to the center of a vinyl-screw bolt in order to minimize the heat loss from the probe to the environment, was placed at the bottom plate (Bakelite plate). The detail of the probe is illustrated in Fig. 4. The thin-wall stainless-steel probe contains a uniformly spaced spiral manganin coil heater (0.2 mm in diameter). The ratio of the length to the diameter of the probe was 100 ($L/D = 100$), so that the probe was considered a line heat source. In order to study the dimensional effect of the probe, four kinds of probes were used, that is, probe diameter $D = 1.5$ mm (heat capacity $\rho c_p = 2.63\ \mathrm{MJ \cdot m^{-3} \cdot K^{-1}}$; thermal diffusivity $\alpha = 1.42 \times 10^{-4}\ \mathrm{m^2 \cdot h^{-1}}$), 2 mm ($\rho c_p = 3.07\ \mathrm{MJ \cdot m^{-3} \cdot K^{-1}}$; $\alpha = 2.71 \times 10^{-4}\ \mathrm{m^2 \cdot h^{-1}}$), 3 mm ($\rho c_p = 3.25\ \mathrm{MJ \cdot m^{-3} \cdot K^{-1}}$; $\alpha =$

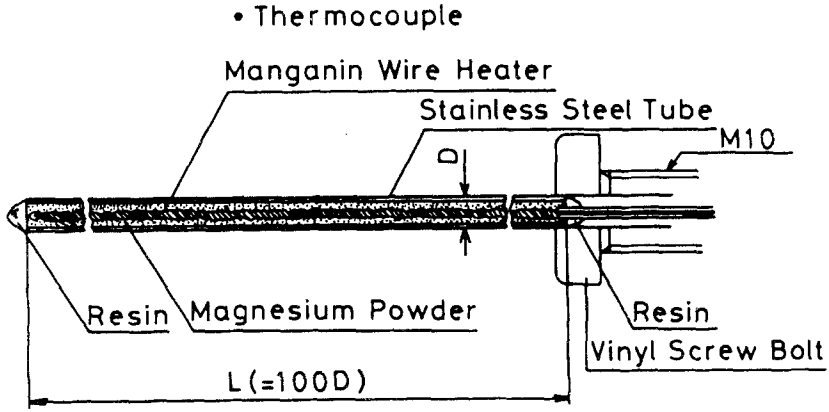

Fig. 4. Detail of the probe used in the transient heat flow method.

3.22×10^{-4} m$^2 \cdot$ h^{-1}), and 5 mm ($\rho c_p = 3.29$ MJ $\cdot$ m$^{-3} \cdot$ K^{-1}; $\alpha = 7.24 \times 10^{-4}$ m$^2 \cdot$ h^{-1}). Alumel–Chromel thermocouples (0.1 mm in diameter) were embedded in the thin stainless-steel probe to measure the surface temperature of the probe. Using fine calibrated thermocouples and a precision potentiometer, the reliability of the temperature measurement was estimated to be within ± 0.04°C. The present apparatus was placed in a temperature-controlled room to minimize thermal disturbances caused by the environment.

The present probes, with a large length-to-diameter ratio ($L/D = 100$), can be considered a line heat source. However, contact points of the particles of the specimen to the probe influence the measured value of the effective thermal conductivity. That is, a void fraction adjacent to the probe causes a measurement error. The temperature at any distance r from the probe surface can be calculated by the following when an air layer having radius a exists around the probe and a geometrically and thermally homogeneous specimen layer is present outside of the air layer.

$$T = T_{in} + \frac{q}{4\pi}\left\{\frac{1}{\lambda_{eff}}\left(\ln\frac{4\alpha_s t}{r^2} - \delta\right) + \frac{1}{\lambda_\alpha}\ln\frac{a^2}{r^2} + \frac{1}{t}\left[\left(\frac{1}{\lambda_{eff}} - \frac{1}{\lambda_a}\right)\frac{r^2}{4\alpha_a} + \frac{a^2}{2}\frac{1}{\lambda_{eff}}\left(\frac{1}{\lambda_{eff}} - \frac{1}{\lambda_a}\right) + \frac{a^2}{2}\left(\frac{1}{\alpha_s\lambda_{eff}} - \frac{\lambda_{aa}}{\alpha_a\lambda_{eff}^2}\right)\left(\ln\frac{4\alpha_s t}{a^2} - \delta\right)\right]\right\} \quad (2)$$

where T_{in} is the initial temperature and subscript s refers to the specimen. If time t is large, the fourth term on right-hand side in Eq. (2) becomes very

small compared with the other terms. Equation (2) can be simplified as follows:

$$T = T_{in} + \frac{q}{4\pi}\left[\frac{1}{\lambda_{eff}}\left(\ln\frac{4\alpha_s t}{r^2} - \delta\right) + \frac{1}{\lambda_a}\ln\frac{a^2}{r^2}\right] \tag{3}$$

Moreover, if the surface temperature of the probe is measured and the air layer becomes very small, Eq. (3) can be expressed as follows:

$$T = T_{in} + \frac{q}{4\pi\lambda_{eff}}\left(\ln\frac{4\alpha_s t}{r^2} - \delta\right) \tag{4}$$

Introducing the temperature difference ΔT ($\Delta T = T_1 - T_2$) between t_1 and t_2, Eq. (4) can be written as follows:

$$\lambda_{eff} = \frac{q}{4\pi\Delta T}\ln(t_2/t_1) \tag{5}$$

For a given specimen, the value of the effective thermal conductivity λ_{eff} was obtained from the least-squares fit to a plot of the temperature change versus the logarithm of the ratio of related times. A typical example of ΔT vs time data which follows closely exponential behavior is shown in Fig. 5. In this figure, the period indicated by ① is dependent on the heat capacity of the probe and the thermal properties of the specimen, and the rate of

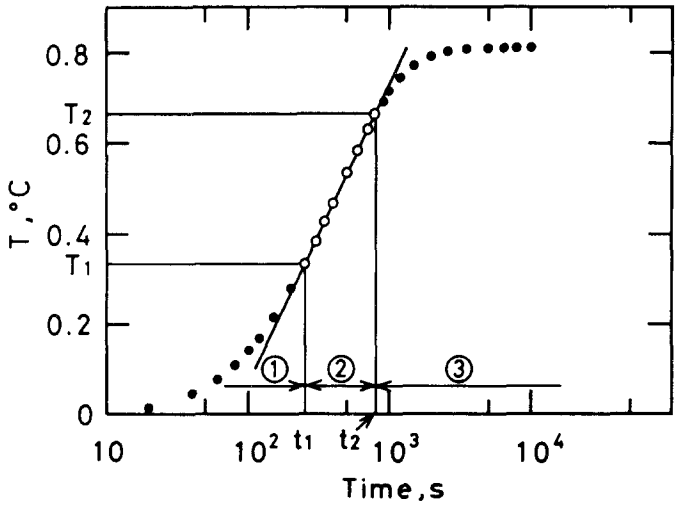

Fig. 5. Typical example of ΔT vs time for the determination of λ_{eff}.

change of temperature with time at $t > t_2$ (region ③) become small due to the occurrence of natural convection in the fluid adjacent to the probe. The temerature difference between time t_1 and time t_2 (region ②) is used to calculated the value of λ_{eff} given in Eq. (5). Based on the preliminary results on water and air, the measurement error in the thermal conductivity measured with the present probes was estimated to be within $\pm 2.5\%$.

3. RESULTS AND DISCUSSION

It is assumed that there exists a geometrically nonhomogeneous layer of particles near the probe because a particle of agriculture material, such as a grain, has only one contact point with the probe surface, whereas it can contact with several other particles in the region away from the probe surface. Figure 6 shows the distribution of local porosity ε in the radial direction when spherical particles are packed around the cyclinder as observed by Kimura et al. [7]. It may be seen that the local porosity ε increases near the wall surface and it becomes constant in the range of $r/d > 0.5$. From this distribution of ε, one can not that contact points of the particles to the probe surface would affect the value of the masured effective thermal conductivity.

The number of contact points of spherical particles to the outside surface of the probe N is calculated by two geometrical models indicated in Fig. 7a. One of the models in the probe length direction is the arrangement of staggered sphere rows as a close packing, as indicated in the left-side model (A) in Fig. 7a. The other is the arrangement of in-line sphere rows as a loose packing in the right-side model (B) in Fig. 7a. The contact points of

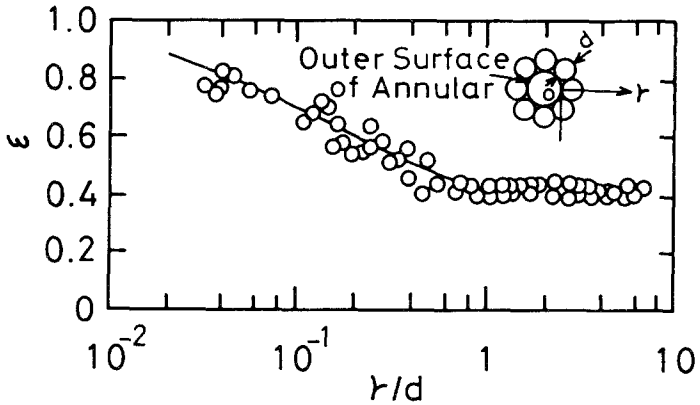

Fig. 6. Distribution of local porosity in the radial direction from the cylinder surface.

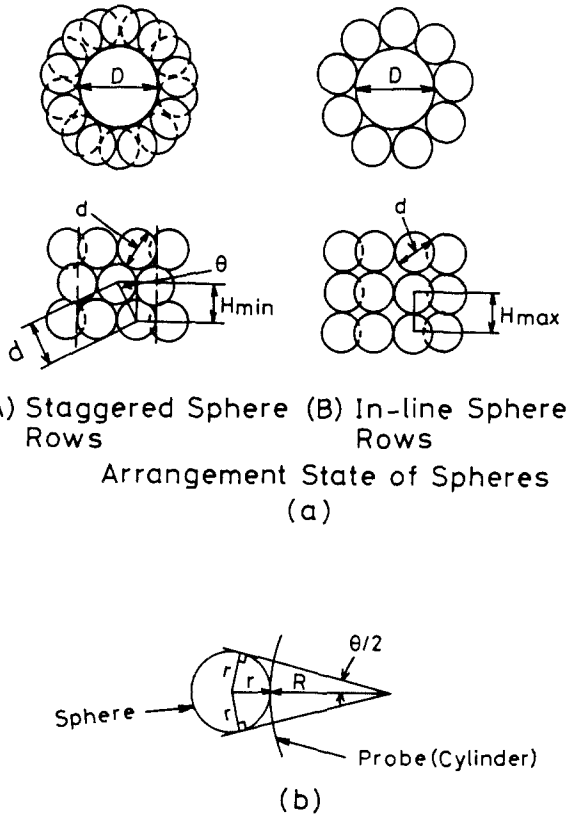

Fig. 7. Calculation model of contact points of the particles of the specimen to the probe: (a) two geometrical arrangements in the probe length direction; (b) geometrical arrangement in the circumferential direction.

spherical particles to the probe in the circumferential direction are calculated from the geometrical arrangement shown in Fig. 7b. Regarding the number of contact points of spherical particles to the probe surface in the probe length direction, the minimum and maximum distances $H_{\min}$ and $H_{\max}$ between two spherical rows as shown in models A and B in Fig. 7a are $\sqrt{3}/2d$ when $\theta = 60°$ and d when $\theta = 90°$ from the equation $H = d \sin \theta$, respectively. Therefore, the total number of contact points N_1 in the probe length direction using probe length L becomes

$$N_1 = L/H = (2/\sqrt{3} \sim 1)L/d \tag{6}$$

where for the number of contact points of spherical particles to the probe surface in the circumferential direction, we can obtain the following equation from the geometrical relation as shown in Fig. 7b:

$$\sin(\theta/2) = r/(R+r), \qquad \text{i.e.,} \qquad \theta = 2\sin^{-1}\left(\frac{r}{R+r}\right) \tag{7}$$

so that the total number of contact points in the circumferential direction N_2 is

$$N_2 = 360°/\theta = 360\Big/\left[2\sin^{-1}\left(\frac{r}{R+r}\right)\right] \tag{8}$$

The total number of contact points of spherical particles to the probe surface is obtained by multiplying N_1 and N_2, which gives

$$N = \left[360/2\sin^{-1}\left(\frac{r}{R+r}\right)\right]\left(\frac{2}{\sqrt{3}} \sim 1\right)\frac{L}{d} \tag{9}$$

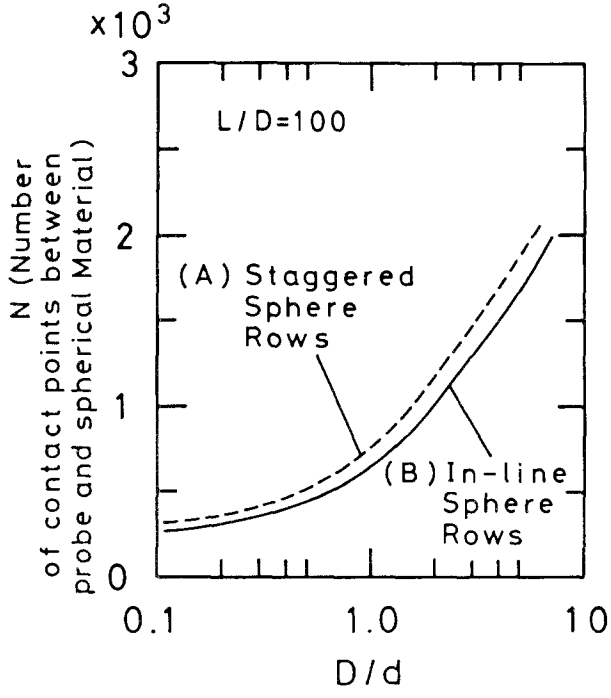

Fig. 8. Variation of the total number of contact points N with the ratio of the probe to the specimen particle diameter D/d.

When the ratio of the probe length to the diameter, L/D, equals 100 in the present study, the value of N can be written by using $m = D/d$ as follows;

$$N = 100m\left[360/2\sin^{-1}\left(\frac{m}{m+1}\right)\right](2/\sqrt{3}\sim 1) \tag{10}$$

Figure 8 presents the relationship between the total number of contact points of spherical particles to the probe N and the ratio of the probe diameter to the diameter of spherical particles D/d for the models A and B, calculated from Eq. (10). From this figure, it can be seen that the increase in N as a function of D/d is small for $D/d < 0.5$ but is rather large for $D/d > 0.5$.

Figure 9 shows the relationship between λ_{eff} measured for four kinds of alumina balls having a large thermal conductivity ($\lambda_s = 15.9$ W·m$^{-1\cdot K}{}_{-1}$) as a standard spherical specimen and D/d for various diameters of the probe. In Fig. 9, the square symbol on the right side indicates the value of λ_{eff} measured by the guarded hot-plane method, and the triangle symbol indicates the value of λ_{eff} calculated by Kunii and Smith's equation [5]. The bar line in the figure indicates the range of the maximum and minimum values measured. It can be seen that the value of λ_{eff} increases with an increase in D/d, and in the range $D/d > 1$ it approaches the values measured by the guarded hot-plane method and calculated by Kunii and Smith's equation [5]. Small values of λ_{eff} for $D/d > 1$ are believed to be due

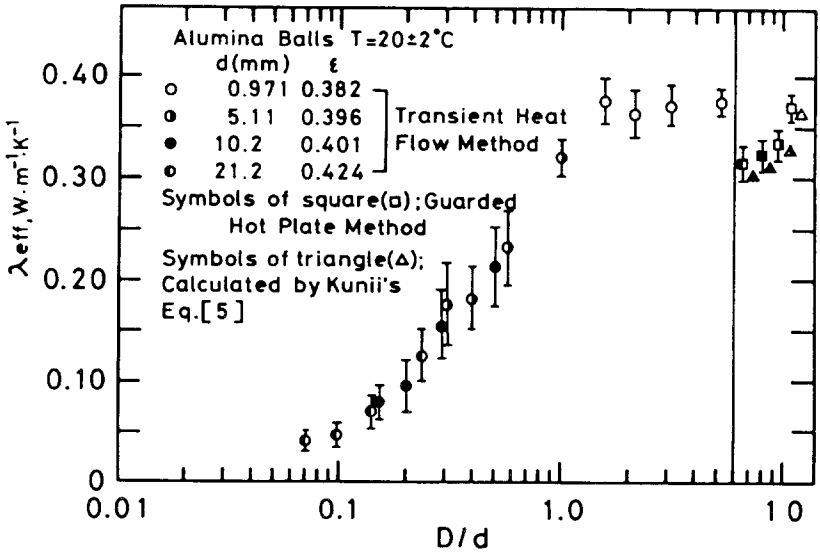

Fig. 9. The relation of the effective thermal conductivity λ_{eff} to D/d for some alumina balls.

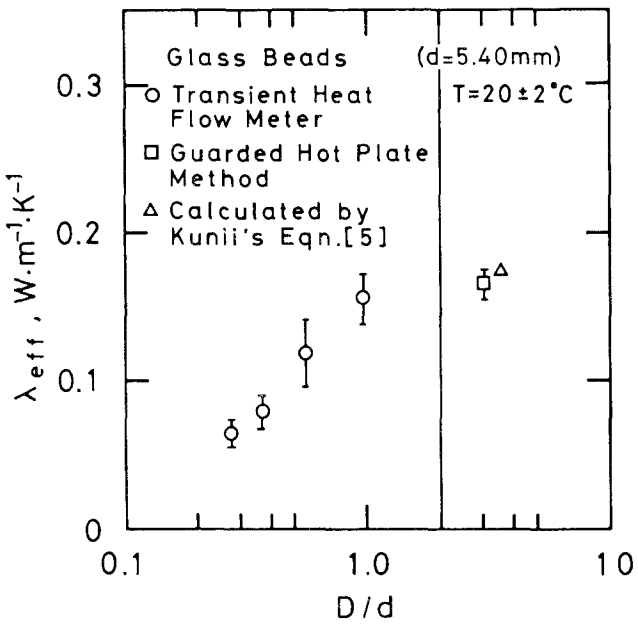

Fig. 10. The relation of effective thermal conductivity λ_{eff} to D/d for glass beads.

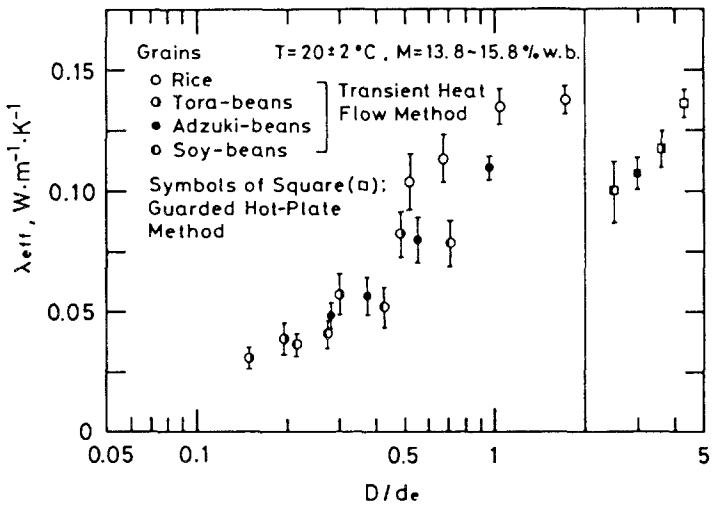

Fig. 11. The relation of the effective thermal conductivity λ_{eff} to the ratio of the probe to the hydrodynamic diameter D/d_e for rice.

to the decrease in the total contact points of particles to the probe in the range of small D/d as shown in Fig. 8, where the air layer having a small thermal conductivity increases near the probe. The relationship between λ_{eff} and D/d for glass beads having a low thermal conductivity ($\lambda_s = 0.74$ $W \cdot m^{-1} \cdot K^{-1}$) is shown in Fig. 10. It may be sen that the variation of D/d vs λ_{eff} for the specimen of glass beads having a low thermal conductivity is similar to that for alumina balls having a high thermal conductivity, since the value of λ_{eff} for the glass beads approaches that measured by the guarded hot-plate method for $D/d > 0.96$. From these results, it can be said that it is possible to measure the effective thermal conductivity λ_{eff} of a specimen of spherical particles when the value of D/d is greater than about unity. Figure 11 shows the reltionship betweeb λ_{eff} and the ratio of the probe diameter to the hydrodynamic diameter D/d_e for some grains. It may be seen that the values of λ_{eff} for the grains measured by the transient heat flow method approach those measured by the guarded hot-plate method for $D/d_e > 0.96$. From these results, one notes that the effective thermal conductivity of grains could be measured by the transient heat flow method when the value of D/d_e is greater than about unity.

4. CONCLUSIONS

It can be concluded that the transient heat flow method utilizing a line heat source can be used for the measurement of the effective thermal conductivity of agricultural materials, such as grains, provided that the ratio of the probe diameter to the hydrodynamic diameter of the particles of the specimen is greater than unity.

NOMENCLATURE

A Area of heating surface
d Diameter of particles of the specimen
d_e Hydrodynamic diameter of particles of the specimen
E Error
H Distance between hot and cold walls
L Probe length
M Moisture content
N Number of contact points of particles of the speciment to the probe surface
Q Net heat flux
q Heat flux per probe length added to probe
R Probe radius
r Radial distance

T Temperature
T_h Surface temperature of the hot wall
T_c Surface temperature of the cold wall
t Time
λ_a Thermal conductivity of air
λ_{eff} Effective thermal conductivity
λ_s Thermal conductivity of a single kernel
α Thermal diffusivity
α_s Thermal diffusivity of a single kernel
ε Porosity
δ Euler constant ($=0.5775...$)
θ Angle

REFERENCES

1. D. Fournier and K. Klarsfeld, *ASRTM STP* **544**:223 (1974).
2. A. Eucken, *VDI-Forsch-Heft* **3**:353 (1932).
3. M. A. Combarnous and S. A. Bories, *Adv. Hydrosci.* **10**:231 (1972).
4. T. Kameoka and S. Okada, *Fifth Jap. Symp. Thermophys. Prop.* **5**:1 (1984).
5. D. Kunii and A. Smith, *AIChE J.* **6**:71 (1960).
6. H. Inaba, *Cold Regions Sci. Technol.* **8**:181 (1983).
7. M. Kimura, K. Nono, and G. Kaneda, *Chem. Eng. (Jap.)* **19**:397 (1955).